Ocean Engineering 102 (2015) 27–39

Contents lists available at ScienceDirect

Ocean Engineering

journal homepage: www.elsevier.com/locate/oceaneng

An elastic–plastic ice material model for ship-iceberg collision simulations

Yan Gao [a], Zhiqiang Hu [a,*,1], Jonas W. Ringsberg [b], Jin Wang [a]

[a] State Key Laboratory of Ocean Engineering, Shanghai Jiao Tong University, Shanghai, China
[b] Department of Shipping and Marine Technology, Chalmers University of Technology, Gothenburg, Sweden

ARTICLE INFO

Article history:
Received 26 September 2014
Accepted 20 April 2015

Keywords:
Ship-iceberg collision
Iceberg material modeling
Elastic–plastic material
Cutting-plane algorithm
Numerical simulation

ABSTRACT

Ship-iceberg collisions are currently a hot topic of research. The modeling of iceberg material is crucial for ice mechanics, and the main objective of the present work is to propose an isotropic elastic–perfectly plastic material model to simulate the mechanical behavior of ice in a ship-iceberg collision scenario for Accidental Limit State conditions. The 'Tsai-Wu' yield surface model and a new empirical failure criterion were used to describe the plastic flow of iceberg material, while a cutting-plane algorithm was adopted to address the plastic stress–strain relationship. The proposed iceberg material model was incorporated into the LS-DYNA finite element code using a user-defined subroutine. Calibration of the proposed material model was conducted through a comparison with an abnormal level ice event pressure-area curve. The calculated pressure-area curve was comparable to that recommended by the International Organization for Standardization (ISO) rule. A sensitivity analysis was then conducted, and the proposed ice model was found to be more sensitive to the mesh size than to other parameters. Numerical simulations of iceberg-tanker side and iceberg-ship bow collisions were also analyzed. Moreover, the impact force and energy dissipation were examined. The results from these simulations showed that the proposed isotropic elastic–perfectly plastic iceberg material model can be employed to simulate iceberg behavior in ship-iceberg collisions under Accidental Limit State conditions.

1. Introduction

More voyages across the Arctic are likely to be possible in the future due to global warming, however, ships are vulnerable to collisions with icebergs in this region. As a result, ship-iceberg collisions are currently a hot topic of research. Accurate collision scenario predictions are necessary for designing ship structures to ensure that ships maintain a sufficient safety level. It is crucial to establish iceberg material models that can be used for realistic representations of iceberg impact loads in ship-iceberg collisions and structural response predictions.

One approach to predicting ship-iceberg impact loads during the ship structure design stage is to use ice class rules, such as the 'Finnish-Swedish Ice Class Rules' (FSICR, 2008) and International Association of Classification Societies (IACS) (IACS, 2011). These rules can be used to calculate the pressure within a ship-iceberg contact area based on parameters that are associated with the ice classification and considered ship structure. Although these references provide a convenient method for predicting collision loads, the current class rules cannot be used to predict ice loads for all collision situations. Considering such limitations, many researchers have adopted numerical simulations to examine ship-iceberg collisions. Ralston (1977) used plasticity theory to describe the ice crushing failure mode, providing a new approach to study the mechanical behavior of ice. Jebaraj et al. (1992) used the finite element method to simulate ship-ice interactions. The ice was considered to be elastic using the 'Tsai-Wu' failure criterion. A failure reference number was adopted to initialize the element failure. In their work, the relationship between the impact velocity and ice failure mode was discussed. They reported that the ice would crush rather than bend under high impact velocity conditions. Jordaan (2001) evaluated the physical properties involved in the interaction of an iceberg with an offshore structure; ranked data from ship rams were used to predict the ice load. von Bock und Polach and Ehlers (2013) proposed a Lemaitre damage model to simulate model-scale ice. The parameters of the material model were based on experimental data. Considering the difference between actual and model-scale ice, it is unclear whether this model is suitable for ship-ice simulations. Using the 'Tsai-Wu' yield function and an empirical failure criterion, Liu et al. (2011b) presented a plastic material model to simulate the ice behavior in ship-iceberg collisions. In addition, the plastic material model was

* Corresponding author. Tel.: +86 21 3420 7053 2131.
E-mail address: zhqhu@sjtu.edu.cn (Z. Hu).
[1] Postal address: State Key Laboratory of Ocean Engineering, Shanghai Jiao Tong University, No.800 Dongchuan Road, Shanghai, China.

http://dx.doi.org/10.1016/j.oceaneng.2015.04.047
0029-8018/

successfully applied to the integrated analyses of ship side and bow collisions (Liu et al., 2011a). The failure criterion developed in this paper is based on the one proposed by Liu. Lubbad and Løset (2011) proposed a real time simulation program to simulate ship navigation in a broken ice field. The ship-ice contact area was calculated using a discrete method, and the nominal contact area was used to replace the actual contact area. Jia et al. (2009) used an isotropic elastic–plastic constitutive material model (including material hardening) to represent the ice material during ship-ice interactions. The material data were derived from the results of experiments. Gagnon (2011) proposed a crushable foam material model to simulate ice with a melted layer. The temperature in the contact surface that was measured in the experiment decreased with time, which is primarily because the melted ice 'absorbs' the heat created by the high-pressure conditions. In Gagnon's model, Poisson's ratio was set to zero to simulate viscous fluid flow. Although there has been substantial work on ice material modeling, no previous material models have perfectly represented all ice characteristics.

A clear understanding of iceberg mechanics in ship-iceberg collisions forms the basis for representing ice by a constitutive material model in ship-iceberg collision simulations using the finite element (FE) method. Iceberg mechanical properties strongly depend on the surrounding environmental conditions, which contribute to the complexity of an iceberg's material characteristics. For example, the ice in the Baltic Sea and around Russia can be very different with each other due to the high levels of fresh water pouring into the marginal seas (Timco and Weeks, 2010). Therefore, icebergs in different regions should be treated separately. The icebergs considered in this paper are located in the Arctic. Apart from environmental conditions, ice has complex components because of its formation and growth processes. Sea ice generally consists of solid ice, brine sells, gas and pores. As ice grows, the percentage and arrangements of these components change substantially, leading to different ice properties (Cole, 2001). Therefore, ice in different stages or ages should be studied separately. According to the World Meteorological Organization (WMO, 1970), the development of ice cover can be briefly separated into six main stages, i.e., new ice, nilas, pancake ice, young ice, first-year ice and old ice. Fig. 1 shows these ice types and the different stages in their development. Crystal arrangement determines whether ice properties are orthotropic or isotropic. Regarding first-year ice, crystals grow faster in the vertical direction than in the transverse direction because of the vertical heat flow. Therefore, first-year ice possesses a typical orthotropic property. Unlike first-year ice, old ice is conventionally treated as an isotropic material (Sanderson, 1988). The icebergs in the Arctic belong to the old ice category; thus, the material model should be isotropic. Other factors, such as ice thickness, also influence ice mechanics. For thin ice, bending and cracking are the dominating failure modes, crushing is the major failure mode for thick ice. Moreover, because of the high homologous temperature of ice, it is a strain-rate-dependent material. If the strain rate is low (mm/s level), creep and micro-cracking dominate the ice behavior; this ice can be treated as a viscous elastic material (Jordaan, 2001). At high strain rates, ice has a typical brittle failure mode. In reality, bergy bits collide with ships at relatively high speeds and correspondingly high strain rates ($>10^{-3}$ /s), therefore, ice can be represented by a linear-elastic constitutive material model (Schulson, 2001). Considering the aforementioned points, an isotropic elastic–plastic material model is proposed to simulate the icebergs in the Arctic. In addition to the above discussion, many other aspects contribute to the mechanical properties of ice. However, proposing a general material that can capture the mechanics of ice in all aspects is a challenging task. Therefore, the main efforts in this study are to simulate the characteristics of ice loads during ship-iceberg interactions.

The pressure-area relationship is generally used to illustrate ice mechanics in ship-ice interactions. Sanderson (1988) presented a plot of the data from literature and field measurements to represent the pressure-area relationship for ship-ice interactions. Masterson et al. (2007) summarized a series of test data and proposed a new pressure-area curve for local pressure. This pressure–area relationship is recommended according to the International Organization for Standardization (ISO) standards (ISO/CD, (2010)). Other scholars, e.g., Chai and Lawn (2007), have made substantial progress in specifying the governing discipline behind Masterson's pressure–area relationship. Palmer et al. (2009) discussed the pressure–area curve using a fracture mechanics approach. According to his explanation, if ice is idealized as an elastic-brittle material, in which its strength can be defined by linear elastic fracture mechanics (LEFM), the area effect can be determined. Currently, the pressure–area relationship is a cornerstone in ice mechanics and is widely used to represent collision loads.

In conclusion, an isotropic elastic–plastic material model is proposed in this paper to simulate iceberg impact loads during ship-iceberg collisions in the Arctic, especially for the Abnormal Limit State (ALS) conditions (ISO/CD, (2010)). Calibration of the proposed ice material model was performed by comparing the pressure–area relationship with that recommended by ISO. Afterwards, a sensitivity analysis of the material parameters was performed to estimate the effects of their properties. Integrated numerical simulations of ship side collisions and ship bow collisions were also conducted using the proposed material model. This model was incorporated into the LS-DYNA finite element code (Hallquist, 2007) using a user-defined subroutine. Therefore, ship-iceberg collisions under ALS conditions can be predicted solely via numerical simulations using the proposed material model. The results can provide technical support for ship structure design, especially in the case of shipping in ice-covered regions.

2. Isotropic elastic-perfectly plastic ice material model

Due to the physical complexity of ice, it is challenging to create a material model that completely captures the behavior of icebergs during collisions. As a result, the primary objective of ice modeling is to simulate the characteristics of iceberg impact loads, contact

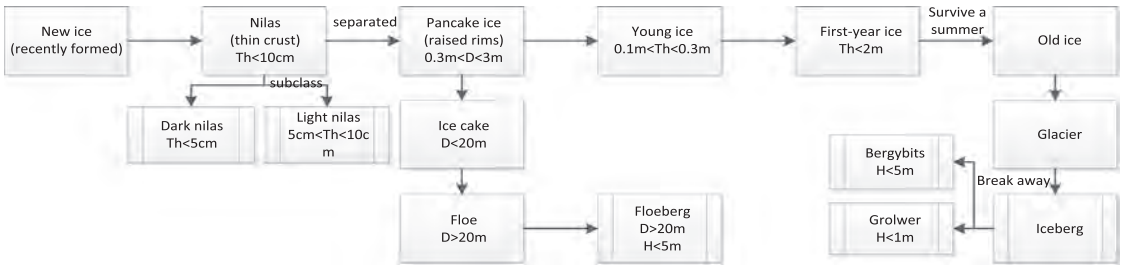

Fig. 1. Ice development stages.

areas and failure criteria. An isotropic elastic–perfectly plastic material model was developed in this study to simulate ice impact loads under ALS conditions. The remainder of this section addresses the development of this material model. First, the basic theory and formula are illustrated; the implementation of the material model in finite element simulations is then discussed. Finally, calibration and sensitivity analyses of the ice material are presented.

Using an isotropic elastic–perfectly plastic ice material model formulation, flow theory is adopted in the constitutive modeling of iceberg behavior. When encountering a ship, ice first undergoes elastic deformation. During this stage, the relationship between the stress and strain satisfies the generalized Hooke's law. Because ship-iceberg collisions are transient dynamic processes, the ice material quickly enters the plastic stage. Once the stress state is on the yield surface, the material transforms into a plastic state. The ice particles in the central contact area are typically highly confined by neighboring particles, indicating that the ice is in a triaxial stress state. Experimental results (Gagnon and Gammon, 1995) have shown that hydrostatic pressure influences the yield mode; for example, the traditional yield function such as the von Mises or Tresa yield functions are not suitable for ice. The tests results reported by Jones (1982) and Rist and Murrell (1994) showed that the yield stress follows an elliptical curve when the q–p plot version is used, where q is the octahedral shear stress and p is the hydrostatic pressure. Considering this issue, the 'Tsai-Wu' (Derradji-Aouat, 2000) yield function is adopted herein:

$$f(p,J_2)=J_2-(a_0+a_1p+a_2p^2)=0, \tag{1}$$

where J_2 represents the second invariant of the deviatoric stress tensor, p is the hydrostatic pressure, and a_0, a_1, and a_2 are constants that require fitting to the triaxial experimental data. In this paper, $a_0=22.93$ MPa^2, $a_1=2.06$ MPa and $a_2=-0.023$; the constant values recommended by Derradji-Aouat (2000) were used. The 'Tsai-Wu' yield function was obtained by fitting approximately 300 experimental data. This yield function has been widely adopted in numerical simulations and calculations of impact loads.

During ship-ice interactions, the ice can be in one of three states (elastic state, elastic–plastic transition state or plastic state) in one load step. The stress tensor of the elastic state can be calculated with the generalized Hooke's law. The analytical solution of the stress tensor cannot be obtained for the other two states. Therefore, an iterative updating algorithm is required to obtain a numerical solution. Considering its high accuracy and simple expression, the cutting-plane algorithm (Simo and Hughes, 1998) was used to calculate the plastic consistency parameter and update the stress tensor state in this study. Using this approach, the plasticity can be mapped back to the yield surface in the finite element simulations.

In a plastic state, the stress continues flowing on the yield surface until the element fails. Consequently, it is important to specify the criterion and process of element failure. If constant variables are adopted (as in this study) and the failure criterion proposed by Liu et al. (2011b) is utilized, the pressure–area curve will be higher than that recommended (Myhre, 2010) for rigid plate-iceberg collision simulations. Therefore, based on the failure criterion proposed by Liu, a new empirical and simple failure criterion is presented in this paper to simulate the behavior of ice failure:

$$\text{if } \varepsilon_{eq}^{p}>\varepsilon_f \text{ or } p<p_c \text{ an element fails,}$$

$$\varepsilon_{eq}^{p}=\sqrt{\frac{2}{3}\varepsilon_{ij}^{p}:\varepsilon_{ij}^{p}},$$

$$\varepsilon_f=\varepsilon_0+\left(\frac{p}{10^8}-0.6\right)^2, \tag{2}$$

where ε_{eq}^{p} is the effective plastic strain, ε_f is the element failure strain, ε_0 is the initial failure strain, which is assumed to be 1% in this study, and p (unit: Pa) is the hydrostatic pressure. If the effective plastic strain exceeds the failure strain or the pressure is less than the cut-off pressure, i.e., p_c, the element fails and its stiffness is immediately set to zero in the numerical simulation.

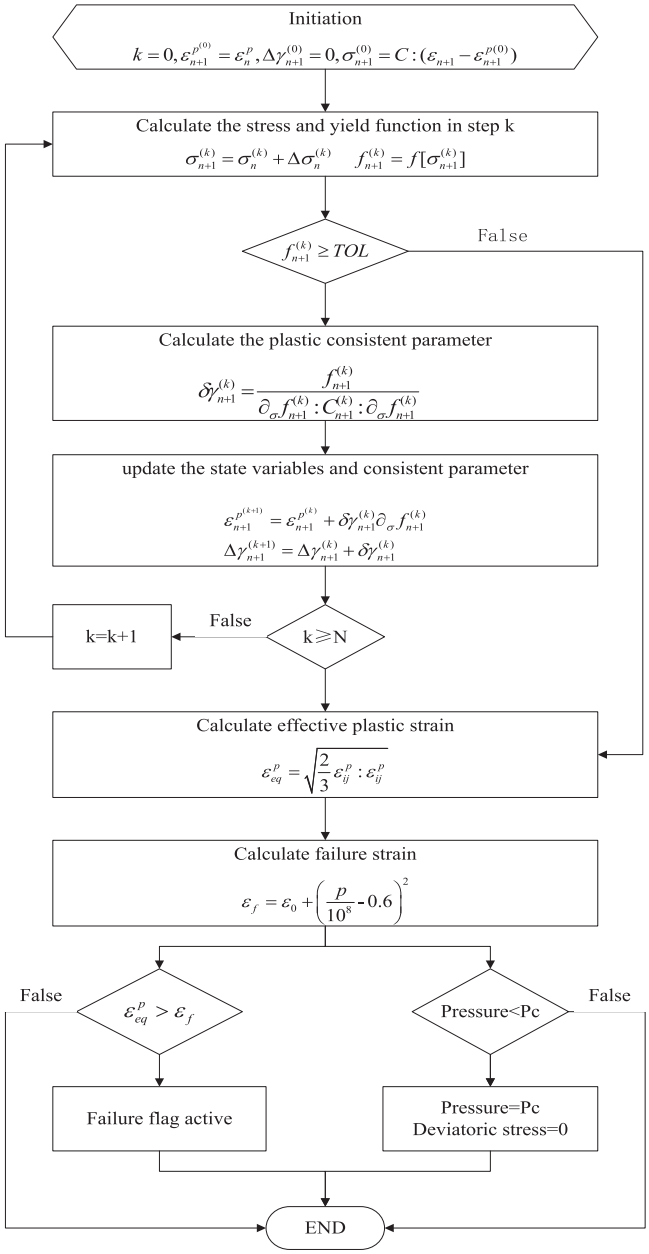

Fig. 2. Framework of the elastic–plastic material model.

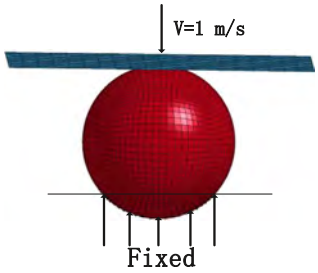

Fig. 3. Spherical ice-rigid plate collision scenario.

Table 1
Iceberg details.

Ice material parameters			
Element type	Solid	Density [kg/m^3]	900
Number of element nodes	8	Poisson's ratio	0.3
Number of element integration points	1	Young's modulus [MPa]	9500
Element length [mm]	50	Cut-off pressure; tension strength [MPa]	2
Strain rate	$>10^{-3}$	Strain hardening function	none
Limit of the elastic strain	10^{-3}	Limit of elastic stress [MPa]	9.5

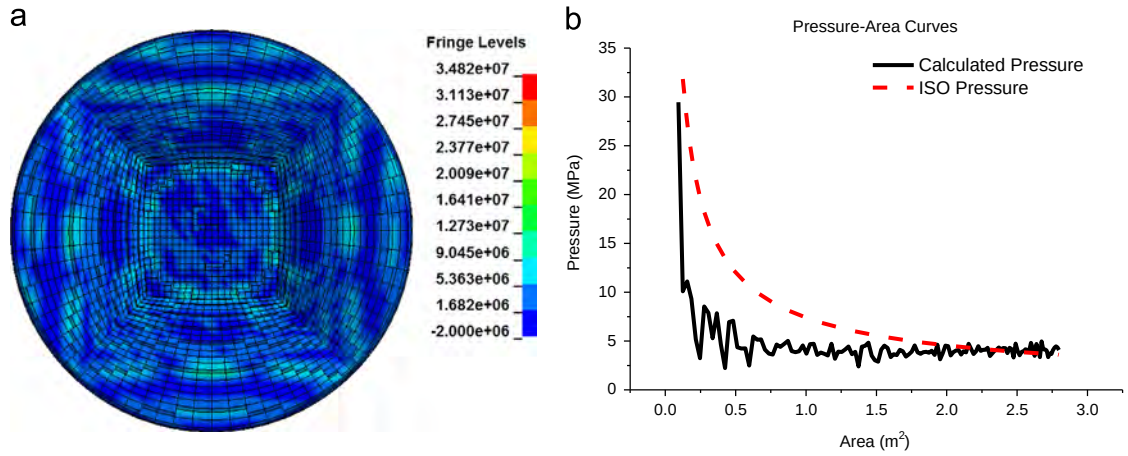

Fig. 4. (a) Contact pressure [Pa] and (b) pressure–area curves.

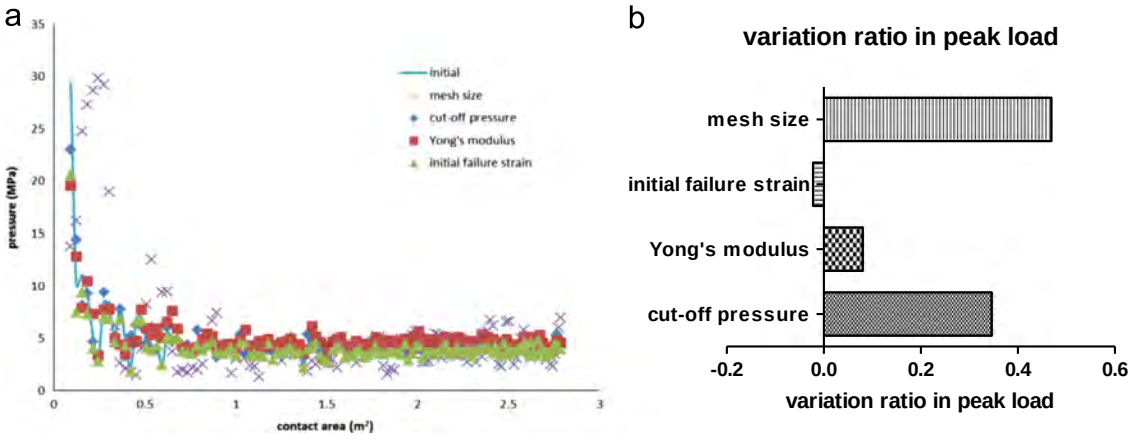

Fig. 5. Sensitivity analysis results; (a) pressure–area curves and (b) variation ratio at peak load.

In summary, an isotropic elastic–perfectly plastic material model was formulated using the 'Tsai-Wu' yield function and a new failure criterion. The framework of the program is summarized in the flowchart in Fig. 2, where k is a control parameter for deciding the number of iterations and N is the maximum number of iterations. In this study, N was set to 10 to ensure completion of the iterative process. The program was incorporated into the LS-DYNA finite element code using a user-defined subroutine.

3. Calibration of the isotropic elastic–perfectly plastic material model

The elastic–perfectly plastic material model was developed for the ALS format. Therefore, the material model should be calibrated against the ALIE curve. For this purpose, a numerical simulation of the rigid plate-iceberg collision was performed; the results of this simulation are discussed in this section. The calculated pressure–area curve was compared with the ISO recommendation for calibration. McKenna (2005) assumed that the mean iceberg model shape could be represented by a sphere. As a result, a spherical iceberg model with a radius of 1 m was chosen. The collision scenario was defined as that in which a rigid plate strikes the spherical ice block with a constant velocity of 1 m/s. This speed was selected to ensure that the ice material had a high strain rate and was also in the range of actual collision velocities. The spherical ice was rigidly fixed at the opposite surface of the collision side (Fig. 3). The computation time was set to 0.7 s, ending when the fixed end of the iceberg model began crushing. Table 1 presents the details of the modeling and representation of ice in the simulations. The limit of elastic strain was

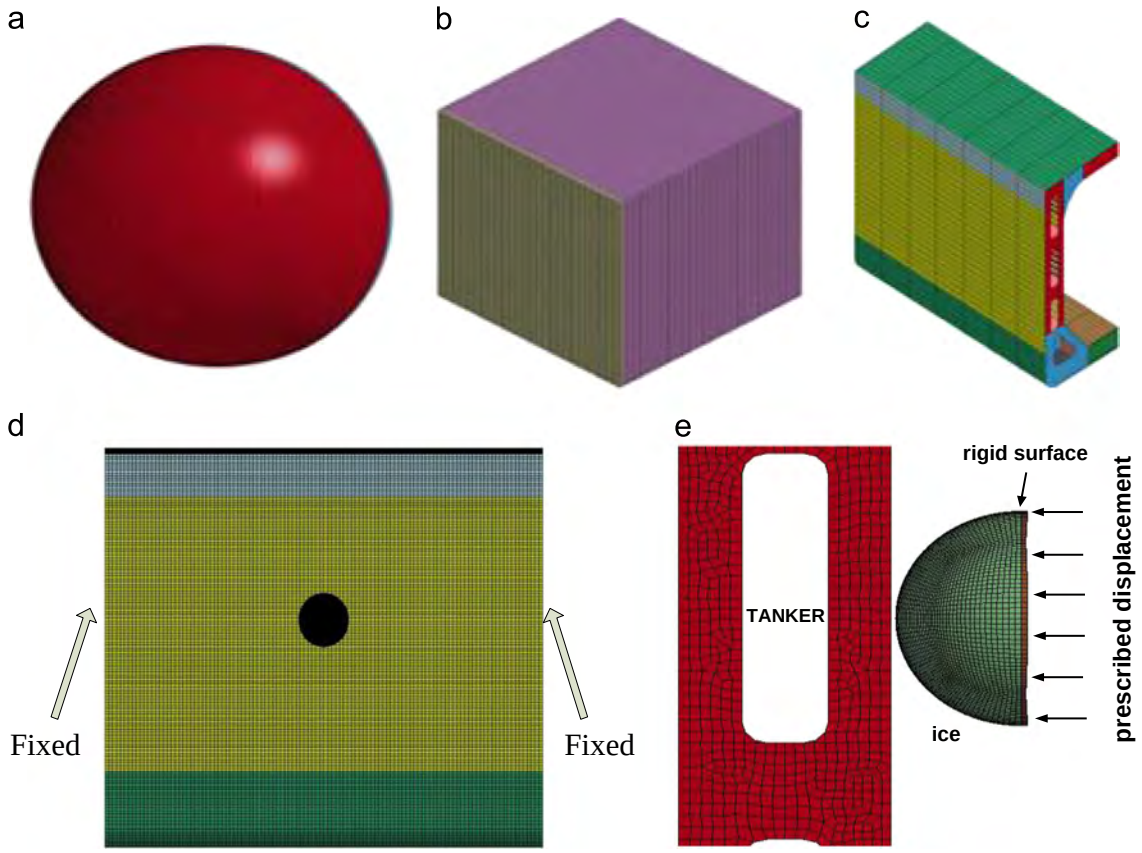

Fig. 6. Iceberg-tanker side structure model and collision scenario.

Table 2
Tanker segment details.

Structure parameters		Material parameters	
Overall length [m]	288	Material	piecewise linear plasticity
Molded breadth [m]	65	Density [kg/m^3]	7890
Molded depth [m]	29.4	Young's modulus [GPa]	2.1
Draft [m]	22	Poisson's ratio	0.3
Side shell spacing [m]	3.4	Yield stress [MPa]	235 (S235)/ 355 (S355)
Outer shell thickness [mm]	20	Failure strain	0.2 (S235)/ 0.15 (S355)
Side stringer thickness [mm]	14	Strain rate parameter P	5
Inner shell thickness [mm]	15	Strain rate parameter C	40.4(S235)/3200(S355)
Segment height [m]	26	Element type	shell
Segment length [m]	35	Typical element dimension [mm]	150
Length between perpendiculars [m]	281	Element number	105664

assumed to be 0.001 for the proposed material model, which was obtained via a single-element test.

Major phenomena that are typically observed in ship-ice collision tests (Gagnon, 2011) include high-pressure zones (HPZs) and low-pressure zones (LPZs) in the contact area. These phenomena have also been observed in spherical iceberg-rigid plate analyses. The contact pressure at the final stage, i.e., $t=0.7$ s, is shown in Fig. 4(a). The maximum pressure in the high-pressure zones was as high as 34.8 MPa, while the average pressure for the low-pressure zones was approximately 2 MPa. The pressure levels in both the HPZs and LPZs were consistent with Gagnon's experimental data (Gagnon, 2011). The transformation between the HPZs and LPZs is constant because of the creation of an impact zone. Furthermore, the elastic–plastic material model was capable of simulating the shattering of ice spalls. Therefore, the iceberg pressure in ship-iceberg collisions can be accurately simulated using the isotropic elastic–plastic material model.

The pressure–area relationship is generally applied to represent ice mechanics during ship-iceberg interactions. According to the NORSOK N-004 (2004) code, structure design can be divided into the following three strategies for the ALS format: *Strength Design, Shared-energy Design and Ductility Design.* If the ice model is capable of predicting a reasonable pressure–area relationship for the *Strength Design* strategy, the material model is considered sufficiently accurate to simulate ice loads during ship-iceberg interactions for the *Shared-energy Design* strategy. Therefore, if the pressure–area curve of a rigid plate-iceberg collision agrees with the ISO rule, the ice material model can be used in ship-iceberg collisions. The isotropic elastic–plastic ice model was subsequently calibrated against the ISO 19906 Arctic Structures Standard (ISO/CD, (2010)). The rule states that the pressure–area relationship satisfies$P_{ISO}=7.4A^{-0.7}$, where P_{ISO} denotes the contact pressure, and A is the contact area. The pressure–area curve and simulation results using the isotropic elastic–plastic ice model are compared in Fig. 4(b). According to the comparison, the pressure–area relationship acquired with the isotropic elastic–plastic material model agrees with the

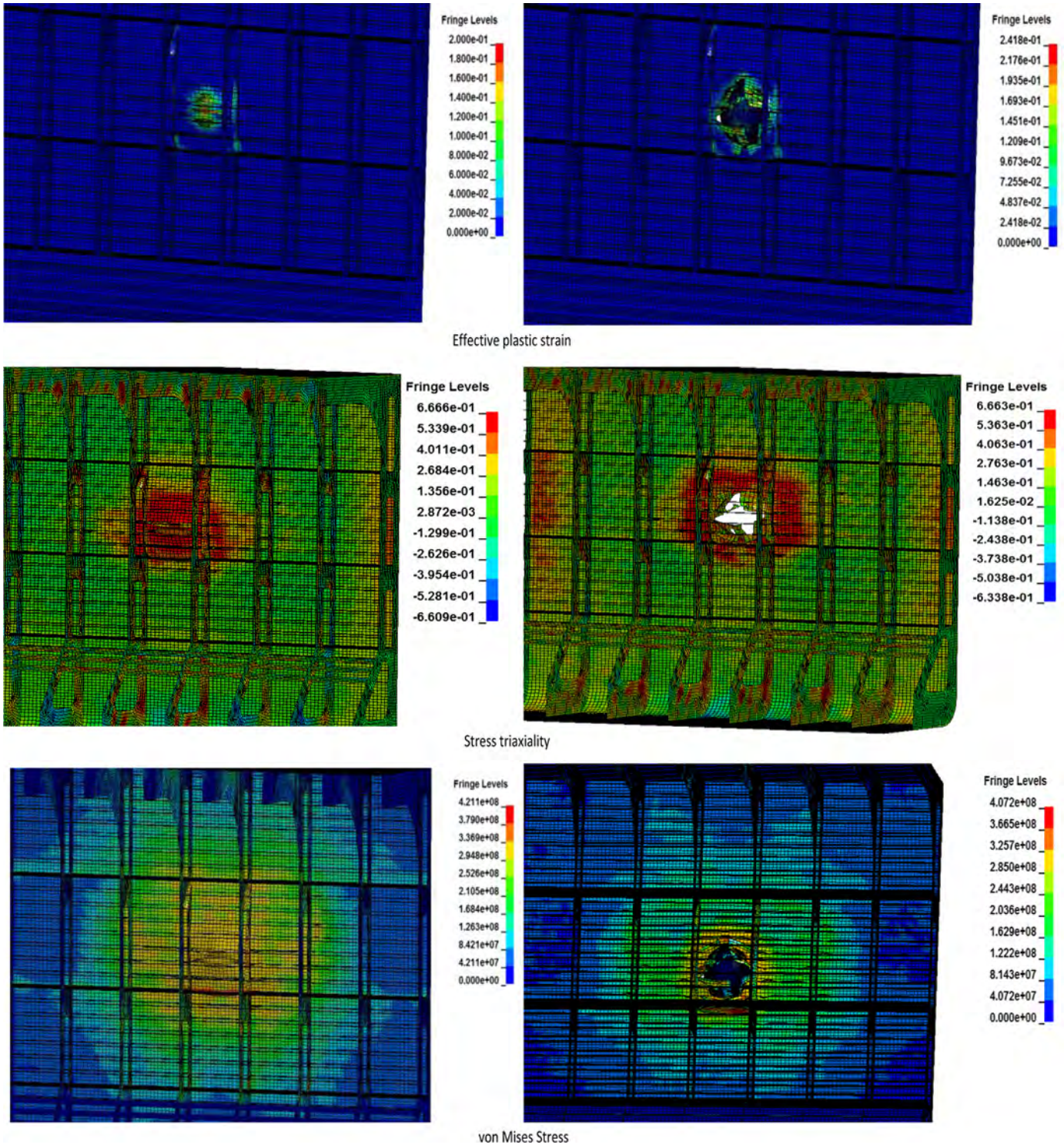

Fig. 7. Collision simulation images (effective plastic strain, stress triaxiality, and von Mises stress[Pa]) at $t=0.5$ s and $t=1$ s.

recommended one for contact areas exceeding 1.5 m^2. Additionally, the high pressure over a small contact area was captured in the numerical simulation. According to the simulation results, the pressure tended to decrease with increasing area, which is consistent with the ISO pressure–area curve. The calculated pressure–area curve was lower than the ISO rule when the contact area was less than 1.0 m^2; hence, further work is needed to improve the model's accuracy. The calculated pressure–area curve exhibits significant fluctuations, which are mainly due to the erosion of iceberg elements. Because rapid changes in the actual contact area will result in contact force oscillation, the pressure oscillates during the initial stage. Moreover, because the contact area remains stable in the later stage, the pressure stabilizes. This calibration demonstrates the accuracy and feasibility of the ice mechanics model calculation algorithm and the solver developed in this study. In conclusion, the isotropic elastic–perfectly plastic ice model can be considered to be valid for the ALS format.

To determine the critical parameters that dominate iceberg behavior during collision events, a sensitivity analysis of the

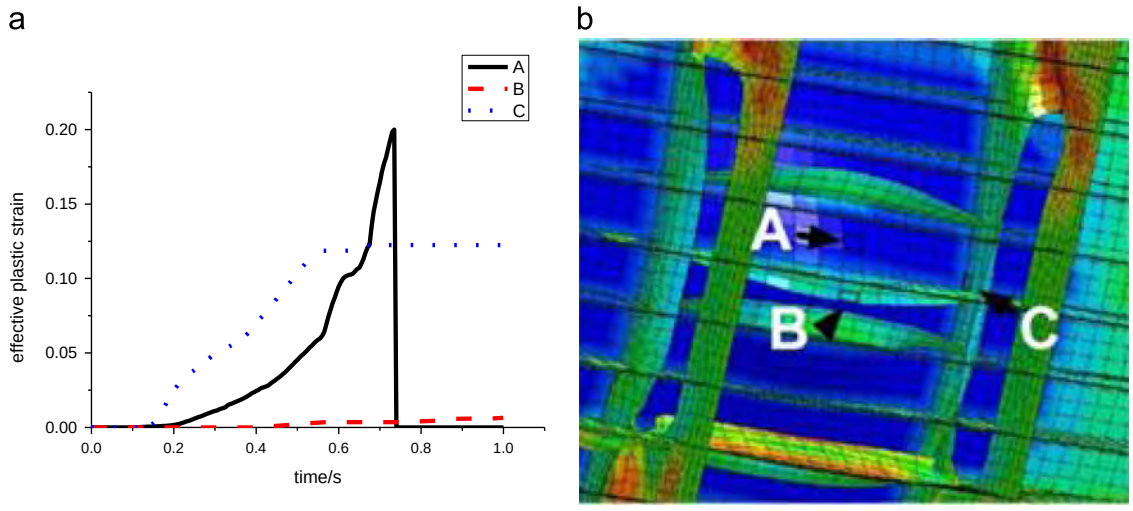

Fig. 8. (a) History of the simulated element effective plastic strain of selected elements and (b) their locations. $t=0.5$ s von Mises stress, $t=1$ s von Mises stress.

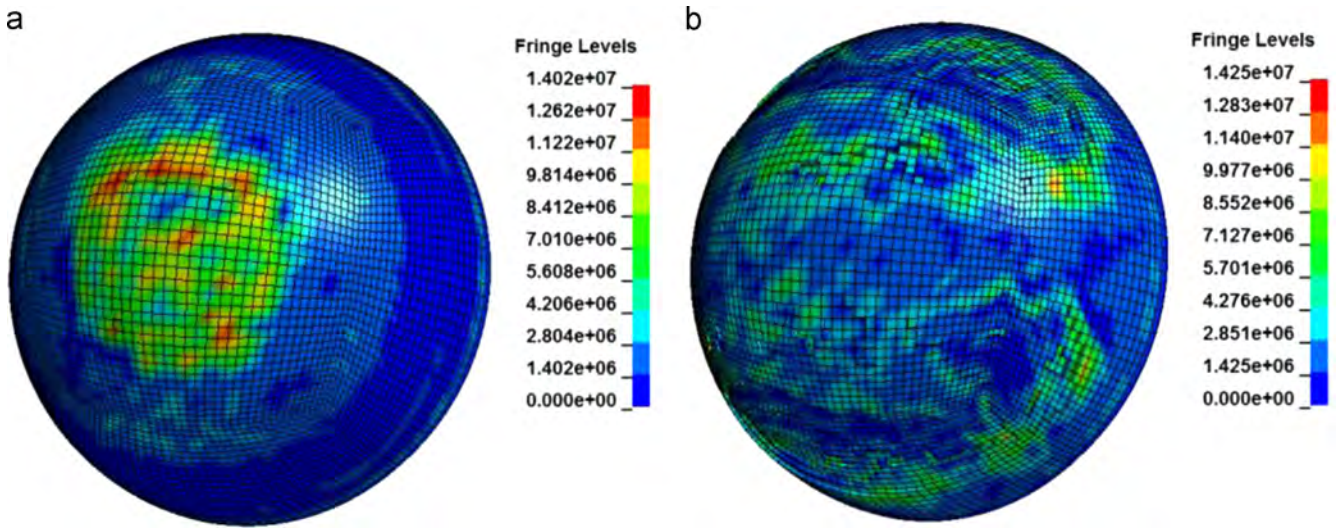

Fig. 9. von Mises stress [Pa] within the spherical iceberg.

following four factors was performed: Young's modulus (9.5 GPa/4.75 GPa), mesh size (50 mm/100 mm), cut-off pressure (-2 MPa/-1 MPa), and initial failure strain value (0.01/0.005) (Kim et al., 2012). Only one parameter was adjusted in each analysis scenario; the other parameters remained constant. The resulting pressure–area curves are summarized in Fig. 5(a), and the ratios relative to the original maximum impact loads are depicted in Fig. 5(b). The pressure–area curves and maximum impact loads were found to be much more sensitive to the ice element mesh size than to the other tested parameters. The variability in the pressure–area curve was more pronounced for the larger ice element mesh size. Therefore, a suitable mesh size is needed to gain a convergent, accurate simulation result. The other parameters, such as the initial failure strain and Young's modulus, had little effect on the ice model characteristics, indicating the stability of the proposed elastic–perfectly plastic material model.

4. Numerical simulations

According to the damage survey conducted by the Finnish and Swedish maritime administrations (Hänninen, 2005), most of the damage caused by floes collisions in the Baltic Sea is small indents on plates in the bow and midship hull area. Therefore, comprehensive tanker side-iceberg and ship bow collision analyses were performed, using the isotropic elastic–perfectly plastic ice model proposed in this paper. First, the collision scenario parameters are presented. Then, the simulation results are discussed and interpreted.

4.1. Tanker side-iceberg collision scenario

In this section, two local iceberg shapes, recommended by DNV (2006), were selected, i.e., a sphere with a radius of 2 m and a cube with a length of 2 m, which are depicted in Fig. 6(a) and (b). A rigid surface was attached to the back of each iceberg model to push the iceberg model forward. Furthermore, the rigid surface was used to simulate the force delivered by the remainder of the iceberg. This collision scenario was selected to represent ice striking the broadside of a tanker with a speed of 2 m/s. The velocity was selected based on the most probable range of collision speeds. The collision duration was set to 1 s. To reduce the computational expense, only the mid-section of the tanker (rather than the entire hull structure) was modeled. Both edges of the tanker sides were fixed at the boundary (Storheim et al., 2012) (Fig. 6(d)). An automatic contact algorithm was adopted for the selected ship-iceberg

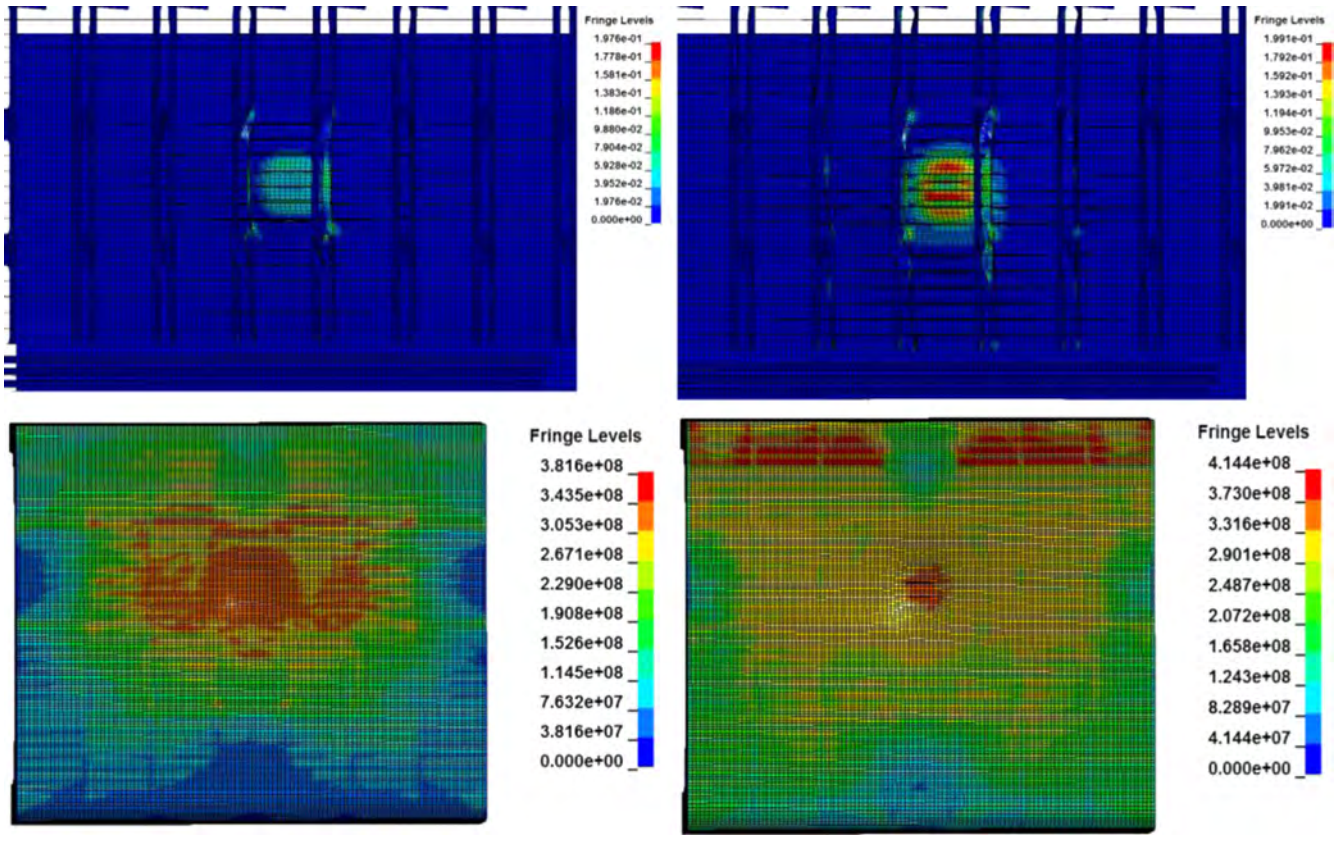

Fig. 10. Effective plastic strain and von Mises stress [Pa] in the ship at $t=0.5$ s and $t=1$ s.

interaction. Moreover, an eroding contact algorithm was utilized for the single iceberg interaction. The static and dynamic friction coefficients were both set to 0.15 in the aforementioned contacts; 'soft option 2' was used to obtain more accurate results. Steel materials, i.e., S235 and S355 (NORSOK N-004, 2004), were applied to the ship side hull. S355 was applied to the upper and lower parts of the tanker side hull; the others parts, including the outer and inner shells, were treated with S235, which was assumed to have a failure strain of 0.2 based on a typical shell element length of 150 mm. The material and element details are summarized in Table 2.

First, the simulated ship-spherical iceberg collision was analyzed. Fig. 7 presents the results for the tanker side structure at $t=0.5$ s and $t=1$ s. The effective plastic strain of the side structure is shown in the first row, which is followed by figures of the stress triaxiality and von Mises stress. As shown in the first row of Fig. 7, the outer shell underwent substantial plastic deformation; the maximum effective plastic strain reached 0.2 at $t=1$ s. Moreover, the outer shell was damaged and was penetrated by the end of the collision. The membrane tensile and tear were the main failure modes of the outer shell. The maximum positive stress triaxiality of the tanker side structure (which was as high as 0.666) was observed at the edge of the contact area. Furthermore, the negative stress triaxiality of the tanker side fluctuated between -0.60 and -0.66. Regarding the von Mises stress of the tanker side structure, the largest stress was observed at the junction of the side stringer and the outer shell (426 MPa). To illustrate the collision more clearly, a time series of the effective plastic strain on three elements at various locations (as shown in Fig. 8(b)), namely the outer shell, frame and stringer, are shown in Fig. 8(a). The effective plastic strain of element 'A' on the outer shell increased until it reached the failure strain; thereafter, the element eroded. Furthermore, the effective plastic strain of element 'B' remained at a relatively low level during the collision, which was probably due to tearing of the outer shell. Element 'B' was pushed away and was no longer involved in the collision process. Regarding element 'C', the effective plastic strain increased before remaining stable at 0.13, indicating that this element did not interact with the neighboring elements in the later collision process. In summary, although the outer shell of the side structure was penetrated, the inner shell remained intact during the collision; therefore, no oil or gas leakage would have occurred in this simulation. However, the ship should be strengthened for voyages in ice-covered region.

With respect to the spherical iceberg model, the von Mises stresses at $t=0.5$ s and $t=1$ s are shown in Fig. 9. Only a few ice elements failed, indicating the high strength of this iceberg model. The ice load was primarily concentrated in critical zones (Fig. 9). These zones are scattered throughout the contact area, which is characteristic of ice mechanics. The largest von Mises stress in the iceberg was 14.3 MPa at $t=0.66$ s.

Second, the ship-cubic iceberg collision simulation was analyzed; the results were slightly different than those of the spherical iceberg simulation. Fig. 10 shows the effective plastic strain and von Mises stress of the side structure due to the cubic iceberg impact at $t=0.5$ s and $t=1$ s. The contact area expanded outward; therefore the distribution of the impact force within the contact area was more homogeneous; excess stress was not observed. As a result, the outer shell remained intact during the collision, which was different from the findings in the former simulation. The maximum effective plastic strain of the side structure was approximately 0.19, and the maximum von Mises stress was 414 MPa. Both values were slightly lower than their counterparts in the previous simulation case.

Similarly, Fig. 11 shows the effective plastic strain and von Mises stress for the cubic iceberg at $t=0.5$ s and $t=1$ s. Unlike the spherical iceberg model, the cubic model appears to be less

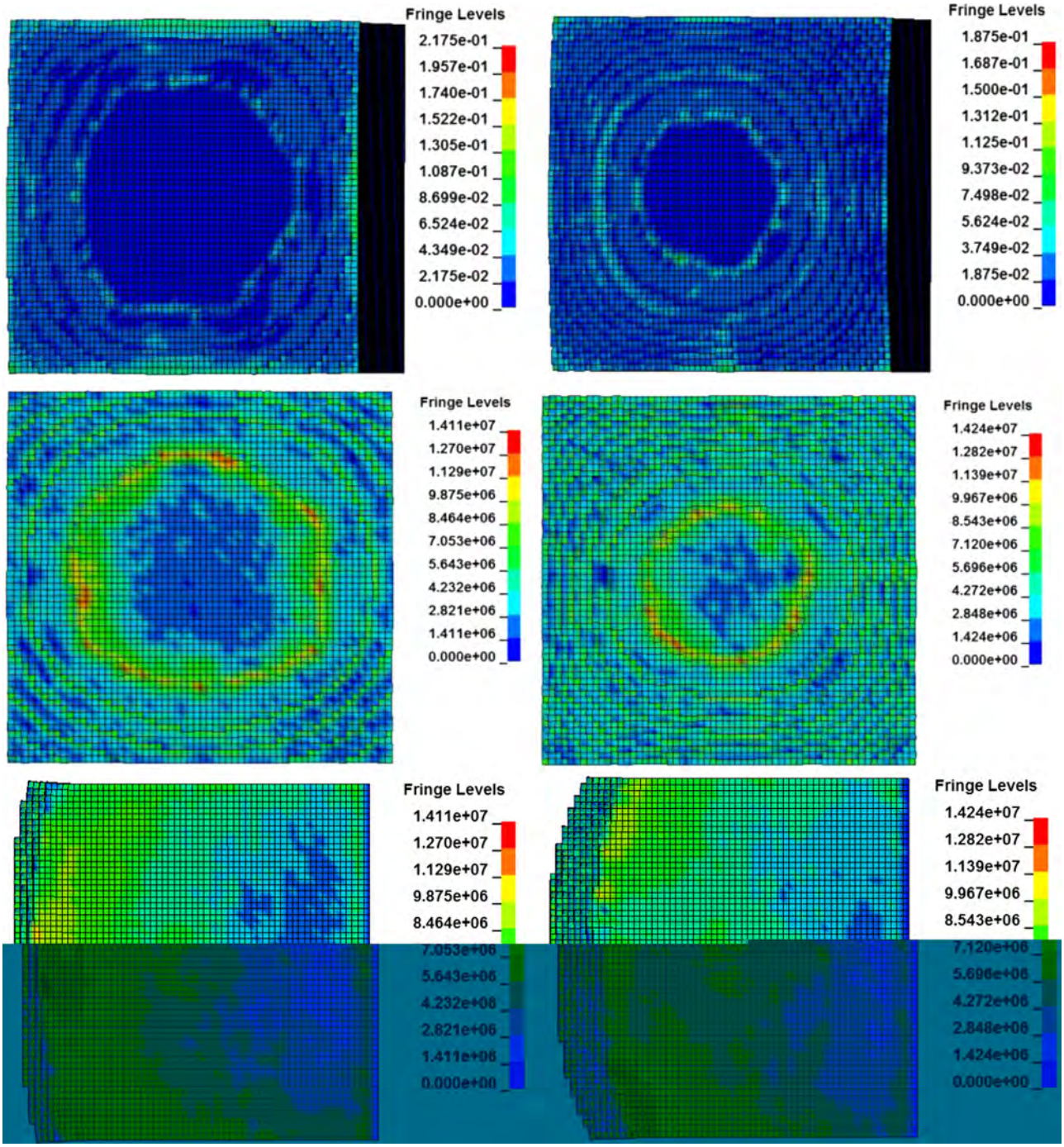

Fig. 11. Effective plastic strain (first row), von Mises stress [Pa] for a front view (second row) and von Mises stress [Pa] for a side view (third row) in the cubic iceberg at $t=0.5$ s and $t=1$ s.

intense with an increasing number of cubic iceberg elements failing during the collision process. Furthermore, the failed elements were primarily found at the edges rather than in the central area, which was not unexpected because the stress is more likely to be concentrated in corners.

To further investigate the feasibility and mechanic characteristics of the isotropic elastic–perfectly plastic material model, the simulated contact force and energy dissipation are presented in Fig. 12. The hull deformation was defined as the largest displacement of the nodes on the hull contact surface. The outer shell was penetrated when the spherical iceberg model was applied; therefore, the curves end after penetration occurred. Based on this definition, the total outer shell deformation was approximately 0.9 m and 2.0 m for the spherical and cubic iceberg cases, respectively. Fig. 12(a) shows the contact forces, which had maximum values of 24.1 MN for the spherical iceberg simulation case and 45.7 MN for the cubic case. Because of the outer shell penetration, the contact force in the spherical iceberg simulation was substantially smaller. Consequently, the maximum value was lower than that of the cubic case. Furthermore, variations in the contact force in the cubic iceberg simulation were noticeable; these oscillations were due to iceberg element failure. In terms of the energy dissipation, there was a slight difference between the two cases. Although the energy dissipated by the iceberg accounted for only a small portion of the total dissipated energy in both cases, the energy dissipated by the cubic iceberg was slightly higher, especially in the later stage of the simulation. The ratios of the energy dissipated by the

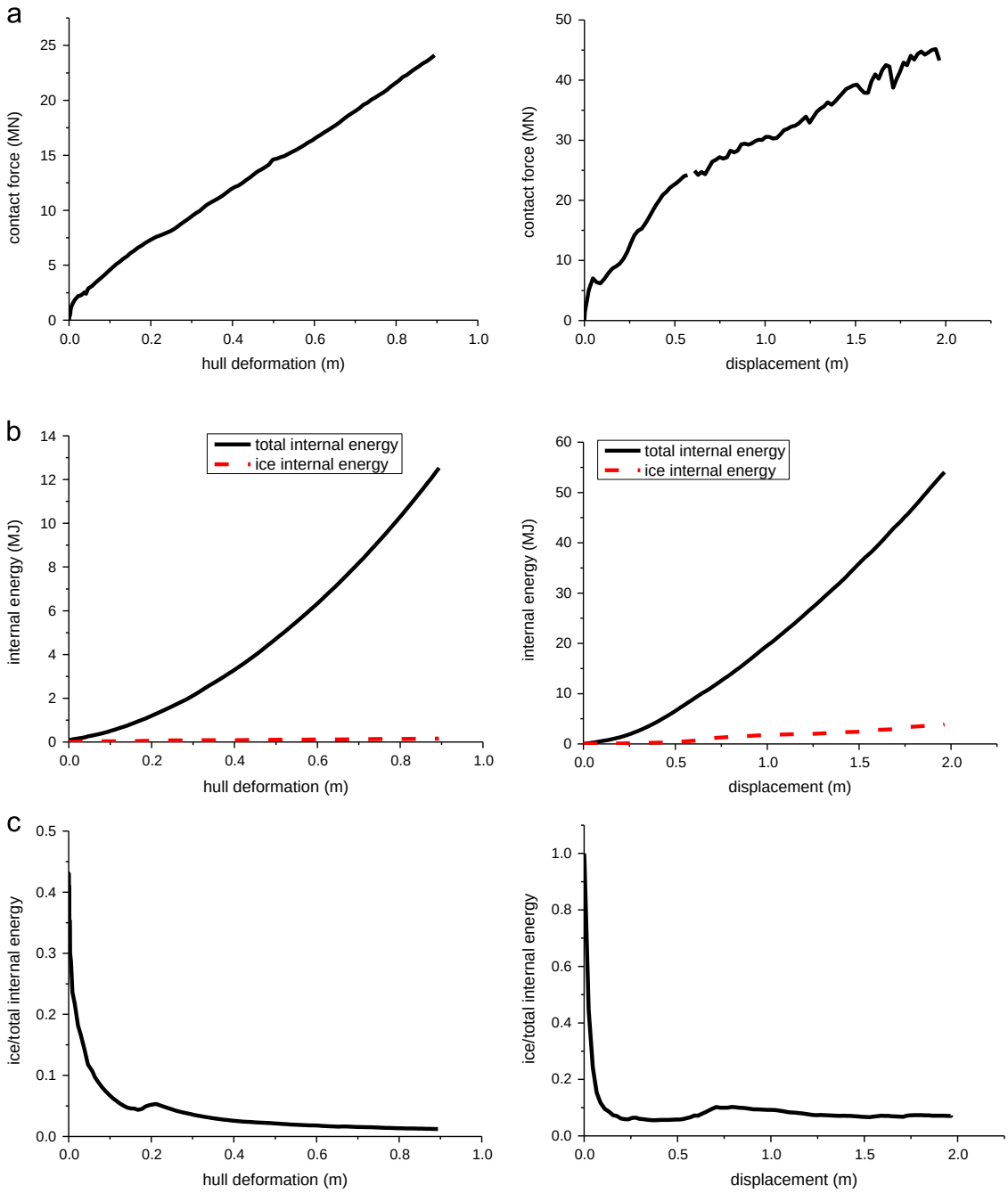

Fig. 12. (a) Contact force, (b) total dissipated energy, energy dissipated by the iceberg and (c) the ratio of the dissipated energy in the ice to the total dissipated energy. (a) Spherical iceberg (left) and cubic iceberg (right), (b) spherical iceberg (left) and cubic iceberg (right), (c) spherical iceberg (left) and cubic iceberg (right).

iceberg to the total energy dissipation were relatively high in the initial stage for both cases, indicating that the ice deformed before the ship structure was altered. Nevertheless, this stage was instantaneous; then, the ratios decreased rapidly, reaching approximately 5% at 0.15 m for the spherical iceberg case and 0.2 m for the cubic iceberg case. The ratios remained at this low level until the end of the simulations. The changes in the ratios indicated that the icebergs deformed first; shortly thereafter, the side structure deformation dominated. The icebergs were hard during the collision, especially for the spherical example.

4.2. Numerical simulation of a ship bow-iceberg collision

A ship bow-spherical iceberg collision was simulated in this study; the results of this simulation are discussed in this section. The iceberg model and collision parameters were the same as those adopted in Section 4.1. S235 steel material was applied for the entire ship bow structure. The collision scenario and inner structure of the ship bow are depicted in Fig. 13. No ice strengthening techniques were applied to the ship bow. The collision point was located at the center of the bulbous bow surface. The collision images at $t=0.5$ s and $t=1$ s are shown in Fig. 14, respectively. Due to sharp bulbous bow edge, a distinct feature that was different from the previous simulations was observed, indicating that the bow only underwent a small deformation. During the ship bow-iceberg interaction, the impact load was concentrated along the edges, leading to high pressure within a small contact area; therefore, many iceberg elements met the failure criterion, leading to removal via erosion. Furthermore, compared to the moderate plastic deformation of the tanker side in the previous simulations, the bulbous bow deformation was relatively small. The deformation

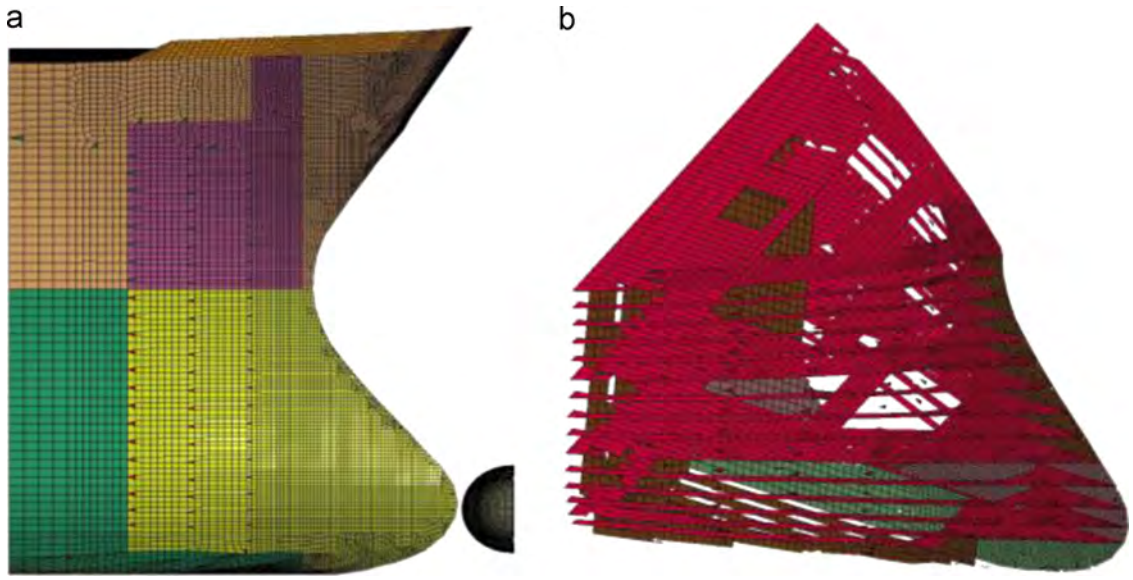

Fig. 13. (a) Ship bow-iceberg collision scenario and (b) ship bow inner structure.

of the bulbous bow was primarily located near the contact surface (Fig. 14). The impact region affected the collision results, especially when the collision occurred at the sharp edges of the hull.

The collision force and energy dissipation are shown in Fig. 15. Regarding the collision force, one of the remarkable points was the oscillatory behavior (similar to the cubic iceberg simulation case). The collision force oscillated through the collision process. The unsteadiness of the collision force was primarily attributed to the failure of the iceberg elements. In elastic–plastic theory, failed elements are unable to handle stress and the contact region is thus scattered. The collision force recovers until a sufficient contact area is reached. As a result, the isotropic elastic–plastic material model proposed in this paper was capable of simulating the characteristics of old ice, which typically has a brittle failure behavior at high strain rates.

In terms of the energy dissipation, the energy dissipated by the ice contributed significantly to the total dissipated energy in the ship bow-iceberg collision due to iceberg crushing. The ratio of the dissipated energy from the ice to the total dissipated energy remained at a high level during the entire collision, and the minimum value was as high as 0.7. This result was found to be quite different from the energy dissipation in the other two simulations. In this case, the strength of the ship bow was larger than that of the ice, indicating a substantially different relative strength relationship.

4.3. Discussion of the numerical simulations

In conclusion, under the condition of the selected ship scantlings and isotropic elastic–perfectly plastic ice material model, an iceberg can indent the plates and spherical icebergs can penetrate the outer shell when impacting the midship region of a ship. Nevertheless, when an iceberg collides with the bulbous bow of the ship, the iceberg is significantly crushed, whereas only slight damage occurs to the ship bow.

The failure criterion used in the isotropic elastic–plastic material was purely empirical, and only one input parameter (ε_0) was needed. More work should be performed to improve its accuracy. In fact, radius and circular cracks may occur when an iceberg is subjected to impact loads. Therefore, a hybrid failure mode can more accurately simulate the ice behavior. Crack propagation was not considered in this study. One way to simulate crack propagation and growth is via cohesive elements instead of finite elements. This technique will be tested in future work. The temperature gradient effect will also be considered in future work. The constant value of the yield function could be assumed for the temperature with linear variations from the surface to the core. The strain rate effect was not considered because there were insufficient related data. Additional work is needed to improve these material models.

5. Conclusions

This paper proposes a specially developed isotropic elastic–perfectly plastic material model for icebergs in the Arctic. Based on the criterion proposed by Liu et al. (2011b), a new failure criterion is presented in the material model to simulate ice failure behavior. This failure criterion depends on the effective plastic strain and hydrostatic pressure. The material model was used for the Abnormal Limit State conditions; therefore, it was calibrated using the design pressure–area curve recommended by the ISO rule in a rigid plate-spherical iceberg simulation case. The calibration showed that this model could capture the important effects governing the mechanical behavior of ice in ship-iceberg collisions. Then, comprehensive ship-iceberg collision simulations were performed using the isotropic elastic–perfectly plastic ice model. The results of the tanker side-spherical iceberg collision and tanker side-cubic iceberg collision were analyzed. Furthermore, the different properties of these two iceberg shapes were investigated. Finally, a ship bow-spherical iceberg collision simulation was conducted. The results were discussed in the context of the contact region effect. The new material model was found to be suitable for the simulation and analysis of iceberg mechanics in ice-ship collision events, especially for the ALS conditions. The model was incorporated into the LS-DYNA finite element code, providing a convenient approach for predicting ice loads in numerical simulations. If the simulation time is set to 1 s, the computation time is approximately 17 h on 8 CPUs. The most important results of this study are as follows:

(1) An isotropic elastic–perfectly plastic material is proposed to simulate the ice mechanics under ALS conditions. The isotropic elastic–perfectly plastic material model was calibrated by comparing the calculated pressure–area curves with the design curve recommended by the ISO rule. The model was successfully applied in the numerical simulations.

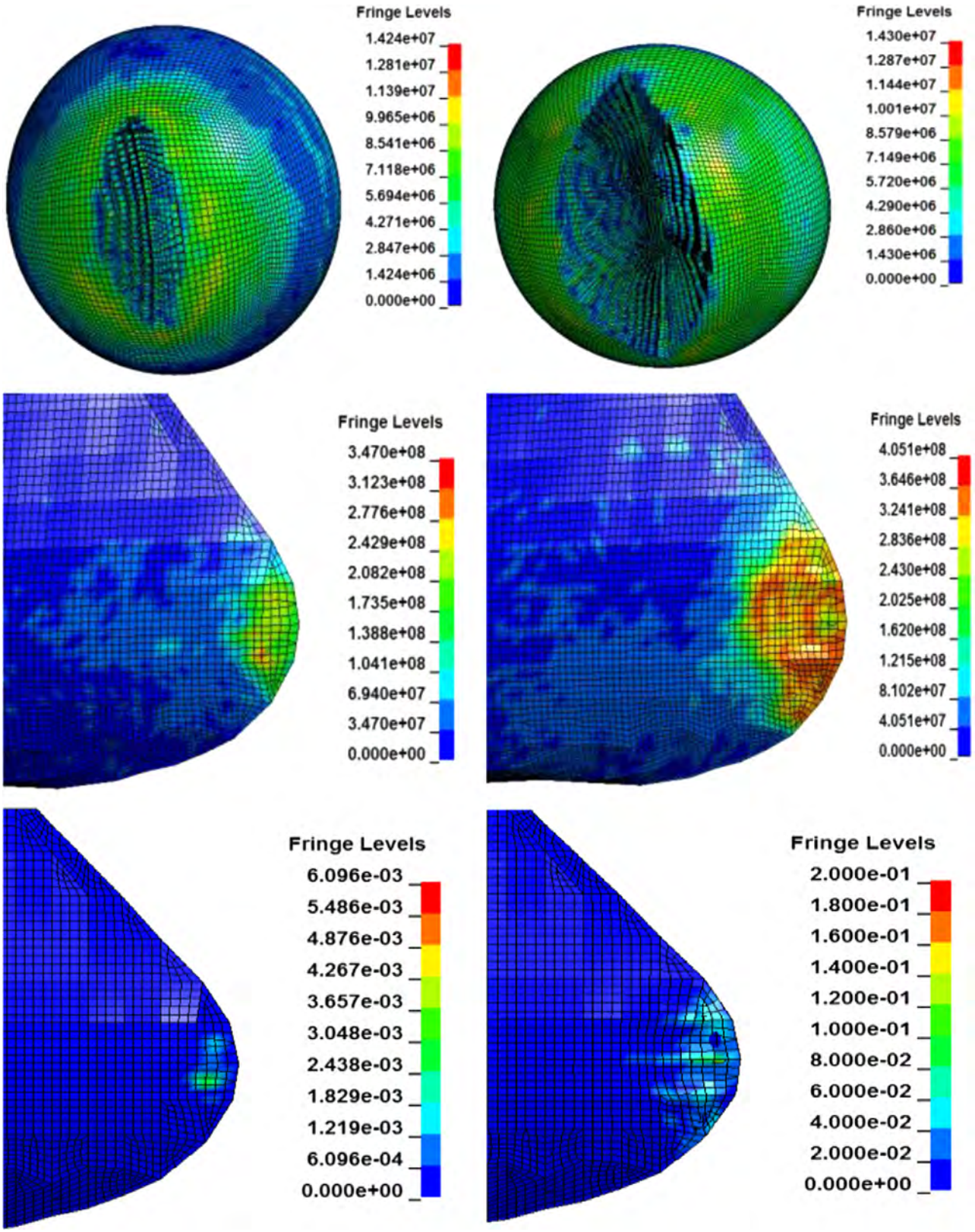

Fig. 14. von Mises stress [Pa] in the spherical iceberg (first row) and ship bow (second row); effective plastic strain in the ship bow (third row) at $t=0.5$ s and $t=1$ s.

(2) The iceberg properties simulated by the isotropic elastic–plastic material model were more sensitive to the ice element size than the other examined parameters, such as the initial failure strain and cut-off pressure.

(3) With respect to the tanker side-iceberg collisions simulated in this study, a spherical iceberg can penetrate the plate. Large deformation of the outer shell was also observed due to the impact of a cubic iceberg. The energy was primarily dissipated

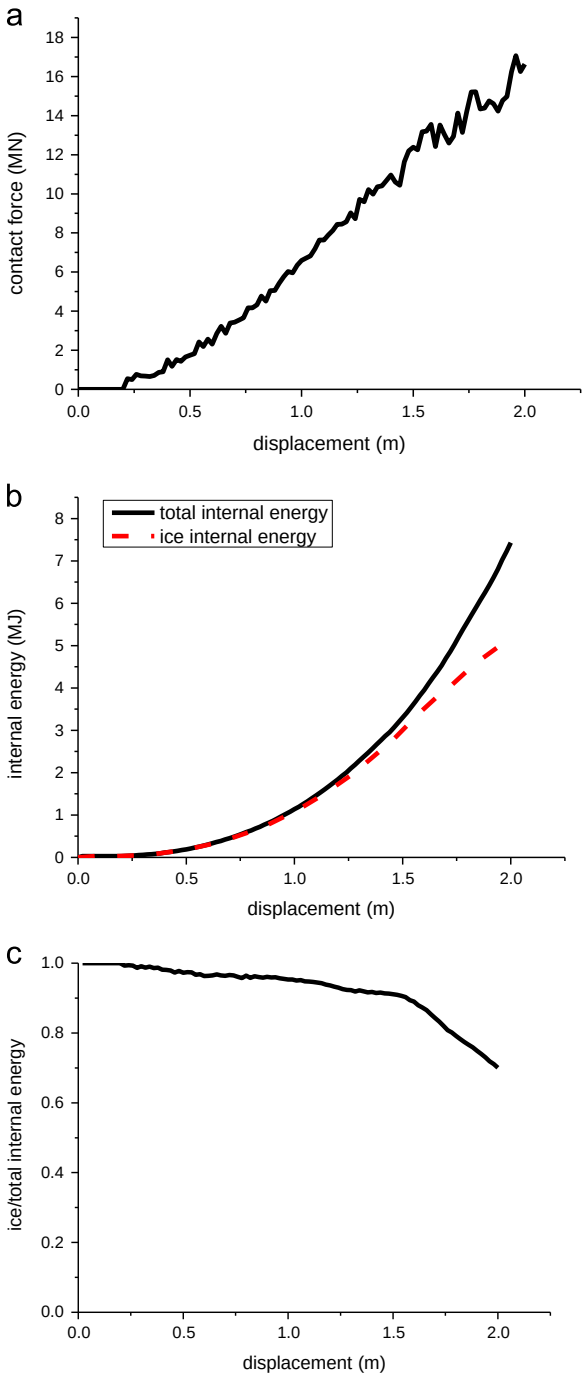

Fig. 15. (a) Contact force, (b) total dissipated energy, energy dissipated by iceberg and (c) the ratio of the dissipated energy in the ice to the total dissipated energy.

by the ship structure. The spherical iceberg was harder than the cubic iceberg.

(4) For the ship bow-iceberg collision simulated in this study, the iceberg crushes due to the sharp edges of the bulbous bow. The ship bow underwent only slight deformation.

Acknowledgments

The work contained in this paper was part of a joint-research project between State Key Laboratory of Ocean Engineering in Shanghai Jiao Tong University and Department of Shipping and Marine Technology in Chalmers University of Technology. Moreover, the Natural Science Fund of China (Grant no. 51239007) supported this collaborative work. The authors greatly appreciate both of these sources of support.

References

Chai, H., Lawn, B.R., 2007. A universal relation for edge chipping from sharp contacts in brittle materials: a simple means of toughness evaluation. Acta Mater. 55 (7), 2555–2561.
Cole, D.M., 2001. The microstructure of ice and its influence on mechanical properties. Eng. Fract. Mech. 68 (17), 1797–1822.
Derradji-Aouat, A., 2000. A unified failure envelope for isotropic fresh water ice and iceberg ice.
DNV, 2006. DNV Technical Report 2006-0672. Ice Collision Scenario.
FSICR, 2008. Finnish and Swedish Ice Class Rules, p. 48.
Gagnon, R., 2011. A numerical model of ice crushing using a foam analogue. Cold Reg. Sci. Technol. 65 (3), 335–350.
Gagnon, R., Gammon, P., 1995. Triaxial experiments on iceberg and glacier ice. J. Glaciol. 41 (139), 528–540.
Hänninen, S., 2005. Incidents and Accidents in Winter Navigation in the Baltic Sea, Winter 2002–2003. Finnish Maritime Administration, Finland.
Hallquist, J.O., 2007. LS-DYNA Keyword User's Manual. Livermore Software Technology Corporation, CA, United States p. 970.
IACS, 2011. Requirements Concerning Polar Class. International Association of Classification Societies, London.
ISO/CD 19906, 2010. Petroleum and Natural Gas Industries-Arctic Offshore Structurs, ISO TC 67/SC 7/WG 8, Final Draft International Standard. International Standardisation Organization, Geneva, Switzerland p. 434.
Jebaraj, C., Swamidas, A., Shih, L., Munaswamy, K., 1992. Finite element analysis of ship/ice interaction. Comput. Struct. 43 (2), 205–221.
Jia, Z., Ringsberg, J.W., Jia, J., 2009. Numerical analysis of nonlinear dynamic structural behaviour of ice-loaded side-shell structures. Int. J. Steel Struct. 9 (3), 219–230.
Jones, S.J., 1982. The confined compressive strength of polycrystalline ice. J. Glaciol. 28, 171–177.
Jordaan, I.J., 2001. Mechanics of ice–structure interaction. Eng. Fract. Mech. 68 (17), 1923–1960.
Kim, E., Storheim, M., und Polach, R.v.B., Amdahl, J., 2012. Design and modelling of accidental ship collisions with ice masses at laboratory-scale. In: Proceedings of the 31st International Conference on Ocean, Offshore and Arctic Engineering. American Society of Mechanical Engineers. ASME, pp. 495–505.
Liu, Z., Amdahl, J., Løset, S., 2011a. Integrated numerical analysis of an iceberg collision with a foreship structure. Mar. Struct. 24 (4), 377–395.
Liu, Z., Amdahl, J., Løset, S., 2011b. Plasticity based material modelling of ice and its application to ship–iceberg impacts. Cold Reg. Sci. Technol. 65 (3), 326–334.
Lubbad, R., Løset, S., 2011. A numerical model for real-time simulation of ship–ice interaction. Cold Reg. Sci. Technol. 65 (2), 111–127.
Masterson, D., Frederking, R., Wright, B., Kärnä, T., Maddock, W., 2007. A revised ice pressure–area curve. In: Proceedings of the Nineteenth International Conference on Port and Ocean Engineering under Arctic Conditions. Dalian, pp. 305–314.
McKenna, R., 2005. Iceberg shape characterization. In: Proceedings of the 18th International Conference on Port and Ocean Engineering under Arctic Conditions. pp. 555–564.
Myhre, S.A., 2010. Analysis of accidental iceberg impacts with membrane tank LNG carriers.
NORSOK N-004, 2004. Design of Steel Structures. Standards Norway, Oslo, Rev 2.
Palmer, A., Dempsey, J., Masterson, D., 2009. A revised ice pressure-area curve and a fracture mechanics explanation. Cold Reg. Sci. Technol. 56 (2), 73–76.
Ralston, T.D., 1977. Yield and plastic deformation in ice crushing failure, Preprint. In: Proceedings of the ICSI/AIDJEX Symposium on Sea Ice-Processes and Models, Seattle, Washington.
Rist, M., Murrell, S., 1994. Ice triaxial deforntation and fracture. J. Glaciol. 40, 135.
Sanderson, T., 1988. Ice Mechanics-Risks to Offshore Structures. Graham & Trotman, London, pp. 1–253.
Schulson, E.M., 2001. Brittle failure of ice. Eng. Fract. Mech. 68 (17), 1839–1887.
Simo, J., Hughes, T., 1998. Computational Inelasticity. Springer-Verlag, New York.
Storheim, M., Kim, E., Amdahl, J., Ehlers, S., 2012. Iceberg shape sensitivity in ship impact assessment in view of existing material models. In: Proceedings of the 31st International Conference on Ocean, Offshore and Arctic Engineering. American Society of Mechanical Engineers. ASME, pp. 507–517.
Timco, G., Weeks, W., 2010. A review of the engineering properties of sea ice. Cold Reg. Sci. Technol. 60 (2), 107–129.
von Bock und Polach, R., Ehlers, S., 2013. Model scale ice—Part B: numerical model. Cold Reg. Sci. Technol. 94, 53–60.
WMO, 1970. World Meteorological Organization Sea-Ice Nomenclature Vol. 1: Terminology and Codes. World Meteorological Organization, Geneva .